

1 **Glyceraldehyde-3-phosphate dehydrogenase subunits A and B are**  
2 **essential to maintain photosynthetic efficiency**

3 Andrew J. Simkin<sup>1,2,\*+</sup>, Mohammed Alqurashi<sup>2,+</sup>, Patricia E Lopez-Calcagno<sup>2,3</sup>, Lauren R.  
4 Headland<sup>2,4</sup>, Christine A. Raines<sup>2</sup>

5 <sup>1</sup> School of Biosciences, University of Kent, Canterbury, United Kingdom, CT2 7NJ, UK.

6 <sup>2</sup> Department of Biological Sciences, University of Essex, Wivenhoe Park, Colchester, CO4  
7 3SQ, UK.

8 <sup>3</sup> School of Natural and Environmental Sciences, Newcastle University, Newcastle upon  
9 Tyne, NE1 7RU, UK

10 <sup>4</sup> School of Molecular Biosciences, University of Glasgow, Glasgow, G12 8QQ, UK

11

12 <sup>+</sup>, These two authors corresponded equally to this work

13 <sup>\*</sup> To whom correspondence should be addressed. E-mail: [a.simkin@kent.ac.uk](mailto:a.simkin@kent.ac.uk)

14

15

16 The author responsible for distribution of materials integral to the findings presented in this

17 article in accordance with the policy described in the Instructions for Authors

18 (<https://academic.oup.com/plphys/pages/General-Instructions>) is: Andrew J Simkin

19 ([a.simkin@kent.ac.uk](mailto:a.simkin@kent.ac.uk)).

20

21 **Short title:** Evaluation of GAPDH subunits A & B in Arabidopsis

22

23

24

25

26

27 **ABSTRACT**

28 In plants, glyceraldehyde-3-phosphate dehydrogenase (GAPDH; EC 1.2.1.12) reversibly  
29 converts 1,3-bisphosphoglycerate to glyceraldehyde-3-phosphate coupled with the reduction  
30 of NADPH to NADP<sup>+</sup>. The GAPDH enzyme that functions in the Calvin Benson Cycle is  
31 assembled either from four glyceraldehyde-3-phosphate dehydrogenase A subunits (GAPA)  
32 proteins forming a homotetramer (A<sub>4</sub>) or from two GAPA and two glyceraldehyde-3-  
33 phosphate dehydrogenase B subunit (GAPB) proteins forming a heterotetramer (A<sub>2</sub>B<sub>2</sub>). The  
34 relative importance of these two forms of GAPDH in determining the rate of photosynthesis  
35 is unknown. To address this question, we measured the photosynthetic rates of Arabidopsis  
36 (*Arabidopsis thaliana*) plants containing reduced amounts of the GAPDH A and B subunits  
37 individually and jointly, using T-DNA insertion lines of GAPA and GAPB and transgenic  
38 GAPA and GAPB plants with reduced levels of these proteins. Here we show that decreasing  
39 the levels of either the A or B subunits decreased the maximum efficiency of CO<sub>2</sub> fixation,  
40 plant growth, and final biomass. Finally, these data showed that the reduction in GAPA  
41 protein to 9% wild-type levels resulted in a 73% decrease in carbon assimilation rates. In  
42 contrast, eliminating GAPB protein resulted in a 40% reduction in assimilation rates. This  
43 work demonstrates that the GAPA homotetramer can compensate for the loss of GAPB,  
44 whereas GAPB alone cannot compensate fully for the loss of the GAPA subunit.

45  
46 **Keywords:** Glyceraldehyde-3-phosphate dehydrogenase; GAPDH; Photosynthesis; biomass

47

48

49 **INTRODUCTION**

50 In recent years there has been a focus to develop strategies to increase crop yields in  
51 order to feed the growing world population against the backdrop of climate change (IPCC,  
52 2014; Pereira, 2017; IPCC, 2019; NASA, 2020). The photosynthetic capacity of a crop over  
53 the season determines the rate of growth and hence yield potential. A number of reports have  
54 now been published demonstrating that under glasshouse and field conditions improvements  
55 in photosynthesis, including the Calvin-Benson Cycle (CBC) can improve the productivity  
56 and yield of the plant (Driever et al., 2017; Kubis and Bar-Even, 2019; Simkin, 2019; Simkin  
57 et al., 2019; Burgess et al., 2022; De Souza et al., 2022; Raines et al., 2022). In the CBC,  
58 glyceraldehyde-3-phosphate dehydrogenase (GAPDH) catalyses the conversion of 1,3-  
59 bisphosphoglycerate to the triose phosphate, glyceraldehyde 3-phosphate (GAP) (Cséke and  
60 Buchanan, 1986). Previous work has shown that the antisense suppression of the GAPDH  
61 gene had no effect on the rate of CO<sub>2</sub> assimilation until GAPDH activity had decreased to 30-  
62 40% of WT levels (Price et al., 1995; Ruuska et al., 2000). However, more recently a study  
63 showed that overexpression of GAPDH in rice (*Oryza sativa*) resulted in increased  
64 photosynthetic CO<sub>2</sub> assimilation under elevated [CO<sub>2</sub>] conditions (Suzuki et al., 2021), raising  
65 the possibility that GAPDH could be a target for future manipulations to improve  
66 photosynthesis.

67 The CBC GAPDH is highly regulated and in plants is comprised of two distinct  
68 subunits, the glyceraldehyde-3-phosphate dehydrogenase A subunits (GAPA) and the  
69 glyceraldehyde-3-phosphate dehydrogenase B subunits (GAPB) that function as either as a  
70 homotetramer A<sub>4</sub> or heterotetramer A<sub>2</sub>B<sub>2</sub> (Cerff, 1979; Iadarola et al., 1983; Howard et al.,  
71 2011). The primary structures of these two subunits show considerable similarity and are  
72 produced from separate nuclear genes (*GapA1*, *GapA2* and *GapB*) (Cerff, 1995). The GAPA  
73 subunits share 92.6% identity and the major difference in the primary sequence between the

74 GAPA and GAPB subunits is a C-terminal extension (CTE) on the GAPB, with substantial  
75 similarity to the C-terminus of Chloroplast protein of 12 kDa (CP12) (Baalmann et al., 1996;  
76 Pohlmeier et al., 1996), This CTE contains cysteine residues which have been shown to  
77 confer thioredoxin-mediated redox regulatory capacity onto the GAPDH A<sub>2</sub>B<sub>2</sub> complex  
78 (Baalmann et al., 1996; Scheibe et al., 1996; Sparla et al., 2002; Marri et al., 2005; Fermani et  
79 al., 2007).

80 In the chloroplast of vascular plants, the predominant active form of GAPDH is  
81 believed to be the A<sub>2</sub>B<sub>2</sub>, however, leaves of many species contain other, less abundant forms  
82 of GAPDH including the A<sub>4</sub> form and the 2(A<sub>2</sub>B<sub>2</sub>) and 4(A<sub>2</sub>B<sub>2</sub>) multimers involved in  
83 deactivation of the enzyme (Wolosiuk and Buchanan, 1976; Scagliarini et al., 1998; Sparla et  
84 al., 2005; Fermani et al., 2007). The homotetramer A<sub>4</sub> form of GAPDH has been termed  
85 'non-regulatory' (GAPDH<sub>N</sub>), firstly because of the absence of the CTE identified in GAPB  
86 and secondly, it fails to aggregate into larger oligomers and the A<sub>2</sub>B<sub>2</sub> regulatory form  
87 (GAPDH<sub>R</sub>) (Scagliarini et al., 1998). In the absence of the CTE, GAPDH<sub>N</sub> is thought to be  
88 regulated by the formation of the CP12/GAPDH/PRK (Phosphoribulokinase) complex (Trost  
89 et al., 2006; Lopez-Calcagno et al., 2014). Although the regulation of the two tetramers of  
90 GAPDH are different, results of Scagliarini et al (1998) showed that the kinetic properties of  
91 GAPDH<sub>N</sub> are similar to GAPDH<sub>R</sub>. The activity data for the GAPDH A<sub>4</sub> and the A<sub>2</sub>B<sub>2</sub> showed  
92 that both of these isoforms have similar kinetic parameters, with a  $V_{max}$  (NADPH) of 130 and  
93 114  $\mu\text{mol min}^{-1} \text{mg}^{-1}$  respectively and a  $K_m$  (BPGA) of 2.0 and 2.3  $\mu\text{M}$  respectively. Based  
94 on these data it was proposed that that the B-subunits are mostly responsible for regulation of  
95 the enzyme (Sparla et al., 2005) and the A-subunits for catalytic activity (Scagliarini et al.,  
96 1998). Over and above the multimers of the A<sub>2</sub>B<sub>2</sub> complex a further level of redox regulation  
97 of GAPDH activity occurs through the formation of a high molecular weight complex which

98 includes the CBC enzyme PRK and the small regulatory protein CP12 (Howard et al., 2008;  
99 Carmo-Silva et al., 2011; Lopez-Calcagno et al., 2014; Lopez-Calcagno et al., 2017).

100 The A<sub>4</sub> homotetramer has been shown in spinach (*Spinacia oleracea*) chloroplast  
101 preparations to constitute 15–20% of the total GAPDH activity (Scagliarini et al., 1998).  
102 Howard et al. (2011) examined stromal extracts from dark-adapted leaves of species from  
103 Leguminosae (pea (*Pisum sativum* ‘Onwards’), Medicago (*Medicago truncatula* ‘Jemalong’),  
104 broad bean (*Vicia faba* ‘The Sutton’), French bean (*Phaseolus vulgaris* ‘Vilbel’)), Solanaceae  
105 (potato (*Solanum tuberosum* ‘Desiree’), tomato (*Solanum lycopersicon* ‘Gardener’s Delight’),  
106 and tobacco (*Nicotiana tabacum* ‘Samson’)), Amaranthaceae (spinach), and the Brassicaceae  
107 (Arabidopsis). This study revealed that the relative amounts of the A<sub>2</sub>B<sub>2</sub> and the A<sub>4</sub>  
108 complexes vary among species. Whereas all species were found to accumulate the A<sub>2</sub>B<sub>2</sub>  
109 heterotetramer, in contrast, in some plant species the A<sub>4</sub> tetramer was not detected (Howard et  
110 al., 2011). This raises the question of the role of the A<sub>4</sub> form for the activity of GAPDH in the  
111 CB cycle. To date the relative importance of the A<sub>4</sub> versus the A<sub>2</sub>B<sub>2</sub> form of plastid GAPDH,  
112 in determining the rate of CO<sub>2</sub> assimilation, has not been elucidated. In this manuscript, to  
113 explore this question we have used insertion mutants in both the *GapB* and *GapA-1* genes  
114 together with transgenic lines where the relative amounts of the GAPA and GAPB proteins  
115 have been decreased individually.

## 116 RESULTS

### 117 Identification and analysis of Arabidopsis lines with reductions in GAPDH A and B 118 transcript and protein levels

119 We identified T-DNA insertion mutants for *gapa-1* (SAIL\_164\_D01) and *gapb*  
120 (SAIL\_308\_A06) from The Arabidopsis Information Resource (TAIR) database  
121 (<http://www.arabidopsis.org/>). All T-DNA insertion sites were confirmed using PCR analysis  
122 of genomic DNA followed by sequencing of the T-DNA/gene junctions. The positions of the

123 T-DNA inserts are presented in **Fig. 1**. Homozygous plants (identified by PCR) were used to  
124 assess the effect of each T-DNA insertion on the expression of the GAPDH transcripts. RT-  
125 qPCR analysis confirmed that the transcript abundance encoding the GAPA subunit in the  
126 *gapa-1* mutant was reduced by approx. 45%, the remaining transcript being produced by the  
127 *gapa-2* gene (**Fig. 2A**). The transcript for the GAPB subunit in the *gapb* mutant was not  
128 detected in the T-DNA insertion line, evidencing the *gapb* mutant as a true knockout (KO)  
129 (**Fig. 2B**). In order to obtain additional independent mutant lines, GAPA and GAPB  
130 expression levels were downregulated using antisense constructs (Supplemental **Fig. S1, Fig.**  
131 **2A and B**). Additionally, two GAPA co-suppressed lines were identified from plants  
132 transformed with a GAPA over-expression construct using the Arabidopsis sequence in the  
133 sense orientation (Supplemental **Fig. S1C**). In *GapA* co-suppressed transformants, we  
134 identified two lines with 5% (cA1) and 11% (cA2) of total *GapA* (*GapA-1* and *GapA-2*)  
135 transcript levels and antisense lines with 35% (aA1) and 11% (aA2) of *GapA* transcript (**Fig.**  
136 **2A**). In anti-sense *GapB* transformants, we identified three lines with 11% (aB1), 15% (aB2)  
137 and 41% (aB2) levels of the *GapB* transcript (**Fig. 2B**). Western blot analysis of these mutant  
138 lines was used to determine changes in GAPDH protein levels, which showed a reduction in  
139 bands at 37.6 kDa representing GAPA and 47.7 kDa (**Fig. 2A and B**). In the GAPA1  
140 insertion line and the GAPA1 antisense lines the level of the GAPA protein was reduced to  
141 51-43% of the CN plants and in the GAPA co-suppressed lines only 9% of the GAPA protein  
142 was detected (**Table 1**). In the GAPB insertion line no band was detected indicating the  
143 absence of the B subunit in this mutant (**Fig.2A**). The level of protein in the GAPB antisense  
144 lines was between 15 and 40% of the CN plants (**Fig.2B and Table 1**).

145

146 **Chlorophyll fluorescence imaging reveals that PSII efficiency is maintained in plants**  
147 **showing a significant reduction in GAPA protein levels.**

148 In order to explore the impact of a decrease in the subunits of the GAPDH enzyme on  
149 photosynthetic capacity, the quantum efficiency of PSII ( $F_q'/F_m'$ ), chlorophyll *a* fluorescence  
150 was analysed (Baker, 2008; Murchie and Lawson, 2013). No significant decrease in  $F_q'/F_m'$   
151 was observed in the *gapa-1* insertion line 164 which had a 45% reduction in *GapA* transcript  
152 levels and 46% reduction in GAPA protein or in the *gapb* insertion line 308 with no  
153 detectable level of the GAPB protein (**Table 1**). The *GapA* antisense lines, containing 46% of  
154 WT protein levels, maintained equivalent PSII photosynthetic efficiency to controls. *GapB*  
155 antisense lines also showed no significant differences in  $F_q'/F_m'$  consistent with the  
156 observed result in the *gapb* insertion line 308, suggesting that in the absence of GAPB, the  
157 presence of the GAPDH A subunit is sufficient to maintain the photosynthetic capacity of  
158 these plants.

159 A small decrease of 12% in  $F_q'/F_m'$  was found in the *GapA* co-suppressed lines that  
160 had the lowest level of GAPA protein (**Table 1**). To investigate further the impact of a  
161 combined reduction of both the GAPA and GAPB protein levels, double mutants *gapa-*  
162 *1/gapb* (164/308) were generated. Homozygous plants with insertions in both *gapa-1* (164)  
163 and *gapb* (308) were grown as described above. Interestingly, double mutants of *gapa-*  
164 *1/gapb* (164/308) showed a significant reduction in  $F_q'/F_m'$  suggesting that a GAPA protein  
165 level of 52% is insufficient to maintain photosynthetic efficiency in the absence of GAPB.

166

### 167 **Photosynthetic CO<sub>2</sub> assimilation and electron transport rates are reduced in lines with** 168 **reduced GAPDH protein level**

169 To assess the impact on photosynthesis of changes in the levels of GAPDH protein,  
170 CO<sub>2</sub> assimilation rates were determined as a function of internal CO<sub>2</sub> concentration ( $C_i$ ) ( $A/C_i'$   
171 curve). Plants were grown in environmentally controlled chambers under short day conditions  
172 as described in materials and methods. The gas exchange measurements were made on

173 mature leaves on plants six weeks after germination.  $A/C_i$  curves were determined for the  
174 *gapa-1* insertion line (164), *gapb* insertion line (308), co-suppressed line of *GapA* (cA),  
175 *GapA* antisense line (aA), *GapB* antisense line (aB) and *gapa-1/gapb* crossed line (164/308)  
176 compared to the controls (CN) plants (**Fig. 3**). From these  $A/C_i$  curves, the maximum rate of  
177 CO<sub>2</sub> assimilation ( $A_{max}$ ) in all mutant lines tested was shown to be significantly lower than for  
178 the CN plants. The plants with the lowest levels of the GAPA protein had the greatest  
179 decrease in assimilation rate (**Fig. 2A**), with maximum assimilation rates attained in these  
180 plants being approx. 27% of that observed in the CN (**Fig. 3A; Table 1**). Furthermore, in the  
181 *gapa-1* mutant (164), an approx. 50% reduction in GAPA protein levels resulted in a 40%  
182 reduction in maximum assimilation (**Fig. 3A**).

183 Plants with no detectable level of GAPB protein (**Fig 2B**) had a 30% decrease in  
184 assimilation rates compared to the 73% reduction observed in a line with 9% GAPA proteins  
185 (cA) (**Fig. 3B**). Finally, in line 164/308, representing the double mutant *gapa-1/gapb*,  
186 containing no GAPB protein and only 51% of the levels of GAPA protein, the assimilation  
187 rates are similar to the single *gapa-1* (164), and *gapb* (308) insertion mutants. This result  
188 suggests that the double mutant shows no cumulative impact on assimilation rates under these  
189 conditions as long as 51% GAPA protein remains (**Fig. 3C**).

190 Further analysis of the  $A/C_i$  curves using the equations published by von Caemmerer  
191 and Farquhar (1981) illustrated that the maximum rate of carboxylation by Rubisco ( $V_{C_{max}}$ )  
192 and maximum electron transport rate ( $J_{max}$ ), were reduced in some lines (Sharkey et al., 2007;  
193 Sharkey, 2016) (Table 1). The results for  $V_{C_{max}}$  showed that lines with a reduction in GAPA  
194 displayed a significant decrease compared to CN. No significant difference in  $V_{C_{max}}$  was  
195 observed in plants with a reduction in GAPB.

196 Furthermore, the results showed that the lines with reductions in either GAPA or  
197 GAPB had a lower rate of photosynthetic electron transport ( $J_{max}$ ), needed to sustain Ribulose



198 1,5-bisphosphate (RuBP) regeneration, when compared to control plants (Table 1). As  
199 previously noted, the maximum rate of CO<sub>2</sub> assimilation ( $A_{max}$ ) was significantly lower in all  
200 lines compared to CN, however,  $A_{max}$  was significantly lower in cA, where *GapA* transcript  
201 and GAPA protein levels were at the lowest levels. No significant differences in  $A_{max}$  were  
202 observed between the single mutants *gapa-1* (164) and *gapb* (308) compared to the double  
203 mutant *gapa-1/gapb* (164/308).

204

### 205 **Growth and vegetative biomass are reduced in both GAPA and GAPB reduced lines**

206 Growth analysis of *GapA* co-suppressed and insertion lines was carried out on  
207 homozygous plants grown in growth chambers at 22 °C under short day length (130  $\mu$ mol m-  
208 2s-1 in an 8 h/16 h light/dark cycle) and relative humidity (RH) 50%. The growth rate of  
209 these plants was determined using image analysis of total leaf area over a period of 52 days  
210 from planting. Observations of the growth rates of *GapA* co-suppressed lines (cA), CN  
211 Columbia (Col-0), and the *gapa-1* and *gapb* insertion lines (164 and 308) showed a  
212 statistically significant reduction in all growth parameters (**Fig. 4**; Supplemental **Fig. S2**).  
213 The co-suppressed and insertion lines were shown to have a statistically significantly slower  
214 growth rate when compared to the CN plants at 40 days post planting (**Fig. 4A and B**). By  
215 52 days post planting, this growth trend continued (**Fig. 4B**) and the final leaf area was  
216 reduced compared to controls (**Fig. 4B**).

217 A growth analysis of the *gapa-1* insertion mutant (164), the *GapA* co-suppressed (cA)  
218 and the *GapA* antisense lines (aA) showed a significant reduction in dry weight and leaf  
219 number (**Fig 5A**) compared to the CN. Significant reductions in the leaf number and final  
220 biomass were seen in the *gapb* insertion mutant (308) and *GapB* antisense lines was also  
221 observed when compared to CN (**Fig. 5B**). A comparative analysis of the single insertion  
222 mutants *gapa-1* and *gapb* with the double mutants *gapa-1/gapb* showed that reduction in

223 both the A and B subunits resulted in a greater decrease in leaf area, biomass and leaf number  
224 after 46 days of growth (**Fig. 5B**), even in the absence of a larger decrease in assimilation  
225 rates observed in **Fig. 3C** (see **Table 1**).

226

## 227 **DISCUSSION**

### 228 **A reduction in GAPA protein levels inhibits CO<sub>2</sub> assimilation and reduces biomass yield**

229 Previous research showed that a 60-70% reduction in GAPDH activity was needed to  
230 affect growth and development in tobacco (*N. tabacum* 'cv W38') antisense GAPDH lines  
231 and that no severe impact on photosynthesis was observed until levels were reduced to less  
232 than 35% of wild-type levels (Price et al., 1995). The results presented in this study clearly  
233 showed a slow growth phenotype in *A. thaliana* following reductions in GAPA protein levels  
234 by 50%. *GapA* co-suppressed lines, with more than a 90% reduction in *GapA* transcript levels  
235 and a barely detectable GAPA protein content showed the most statistically significant  
236 impact on photosynthetic efficiency (-73%) even with GAPB being present at wild-type  
237 levels. The principal form of GAPDH in plant chloroplast has been proposed to be the  
238 heterotetrameric A<sub>2</sub>B<sub>2</sub>. In some plants, including spinach, an A<sub>4</sub> homotetramer has also been  
239 detected representing up to 20% of total GAPDH activity (Scagliarini et al., 1998). This A<sub>4</sub>  
240 homotetramer was not detected in Arabidopsis by previous studies (Howard et al., 2011),  
241 providing evidence that under normal circumstances the A<sub>2</sub>B<sub>2</sub> tetramer is the principal active  
242 form in Arabidopsis. In this study, plants showing an absence of GAPB protein in the *gapb*  
243 mutant lines-maintained photosynthesis rates at 66% of wild type levels suggesting that under  
244 conditions where GAPB is limiting, or absent, that the A<sub>4</sub> form of GAPDH can maintain  
245 photosynthesis.

246 Importantly, the work here also allowed a comparative analysis between plants with  
247 different levels of the GAPA and GAPB subunits under the same environmental conditions.

248 When the *gapa-1* (164) and *gapb* (308) mutant lines were crossed to form the double mutant  
249 *gapa-1/gapb* (164/308), the combined effects resulted in a cumulative reduction in biomass (-  
250 60%), which was significantly greater than the reductions observed in the *gapa-1* (-35%) or  
251 *gapb* (-16%) mutants alone. Interestingly, the assimilation rates for the *gapa-1/gapb* double  
252 mutant showed no further reductions compared to *gapa-1*, and *gapb* single mutants. Firstly,  
253 suggesting that GAPA, even though reduced in level, is able to maintain the assimilation rate  
254 even in the absence of GAPB and secondly, that the decrease in biomass observed in the  
255 double mutant may be due to impacts early in development leading to a cumulative effect on  
256 growth.

257 Recent reviews of the literature have shown that over-expressing of some CBC enzymes  
258 can lead to increases in photosynthesis and biomass and that a multi-target approach can result  
259 in cumulative yield gains in some plants (Simkin, 2019; Simkin et al., 2019; Raines, 2022). The  
260 co-overexpression of *GapA* and *GapB* in transgenic rice increased GAPDH activity to more than  
261 3.2-fold of the wild-type levels; under elevated [CO<sub>2</sub>], CO<sub>2</sub> assimilation increased by  
262 approximately 10% demonstrating that the overproduction of the chloroplast GAPDH proteins is  
263 effective at improving photosynthesis at least under elevated [CO<sub>2</sub>]. However, under these  
264 conditions, no statistically significant differences in biomass were observed compared to wild-  
265 type plants, although a small increase in starch accumulation was observed. (Suzuki et al.,  
266 2021). In contrast, no statistically significant difference in CO<sub>2</sub> assimilation was observed in  
267 ambient [CO<sub>2</sub>] (Suzuki et al., 2021). These results suggest that the manipulation of GAPDH  
268 activity may have more importance as atmospheric [CO<sub>2</sub>] increases due to current climate  
269 change models where [CO<sub>2</sub>] increases from 416 ppm to 550 by 2050 and 700 ppm by 2100 (Le  
270 Quéré et al., 2009; IPCC, 2019; NASA, 2020). Furthermore, given that no increase in growth  
271 rate or final biomass was observed at ambient [CO<sub>2</sub>], increasing GAPDH may have more value

272 in a multi-target approach, such as targeting additional CBC enzymes, photorespiratory elements  
273 and photosynthetic electron transport in combination with GAPDH in the same plants.

274

## 275 **CONCLUSION**

276 Our results have shown that both GAPA and GAPB are essential for normal growth  
277 and development in Arabidopsis plants and that the A<sub>2</sub>B<sub>2</sub> form of the enzyme is required for  
278 maximum photosynthetic efficiency. The phenotypes described in this manuscript provide *in*  
279 *vivo* evidence of the relative importance of the individual subunits of the GAPDH complex  
280 on photosynthetic carbon assimilation. In this study we also show that the suppression of  
281 GAPA to almost undetectable levels resulted in a 73% decrease in carbon assimilation  
282 compared to 34% reduction in photosynthesis in the absence of GAPB providing direct  
283 evidence of the importance of GAPA in maintain photosynthetic capacity.

284

## 285 **MATERIALS AND METHODS**

### 286 **Identification and analysis of T-DNA GAPDH mutants and production of double** 287 **mutants**

288 The *gapa-1* and *gapb* mutants in Arabidopsis (*Arabidopsis thaliana*) were identified  
289 in the Arabidopsis Information Resource (TAIR) database (*gapa-1*: SAIL\_164\_D01 and  
290 *gapb*: SAIL\_308\_A06). The mutant insertion sites were identified by PCR and the location of  
291 each T-DNA insertion was determined by sequencing the PCR products spanning the  
292 junction site (**Fig. 1**). The *GapA-1* was amplified with forward primers GapA1 Fwd  
293 (5'gagagcatgtgacataacggg'3) and reverse primer GapA1 Rev (5'accttaagcttggcctcagtc'3) in  
294 conjunction with primer Sail\_LB3 (5'tagcatctgaatttcataaccaatctcgatacac'3). The *GapB* was  
295 amplified with forward primers GapB Fwd (5'cgacgatgtctcctctcage'3) and reverse primer  
296 GapB Rev (5'gaccgggattcttgagacg'3) in conjunction with primer Sail\_LB3. Double mutants

297 *gapa-1/gapb* (164/308) was obtained by crossing homozygous plants of *gapa-1*  
298 (SAIL\_164\_D01) and *gapb* (SAIL\_308\_A06) and segregating the double homozygous  
299 plants.

300

### 301 **Construct Generation**

#### 302 *GAPA and GAPB antisense constructs*

303 A partial-length coding sequence of glyceraldehyde-3-phosphate dehydrogenase A subunit  
304 (*GapA-1*: At3g26650) and the glyceraldehyde-3-phosphate dehydrogenase B subunit (*GapB*:  
305 At1g42970) were amplified by RT-PCR using primers AtGAPAf  
306 (5'cacctatcgaaggaaccggagtgt'3) and AtGAPAr (5'tcctgtagatgttgaacaatg'3) and AtGAPBf  
307 (5'caccttgatggtaagctcatcaaagtt'3) and AtGAPBr (5'ggtgtaggagtgtgtggtt'3) respectively. The  
308 resulting amplified products were cloned into pENTR/D (Invitrogen, UK) to make pENTR-  
309 GAPA1; pENTR-*antiGAPA* and pENTR-*antiGAPB*. The cDNA's were introduced into the  
310 pGWB2 gateway vector (Nakagawa et al., 2007 AB289765)) by recombination from the  
311 pENTR/D vector to make pGWB2-AntiGAPA and pGWB2-AntiGAPB (Supplemental **Fig.**  
312 **S1**). cDNA are under transcriptional control of the 35s tobacco mosaic virus promoter, which  
313 directs constitutive high-level transcription of the transgene, and followed by the *nos* 3'  
314 terminator.

315

#### 316 *GAPA-1 sense constructs*

317 Destination vector pGWPTS1 was generated as described in Simkin et al., (2017).  
318 The full-length coding sequencer of *GapA-1* was amplified using primers AtFwd  
319 (5'caccatggcttcggttactttctctgtcc'3) and AtRev (5'ttgatgaaatcacttccagttgttgg'3). The resulting  
320 amplified product was cloned into pENTR/D (Invitrogen, UK) to make pENTR-AtGAPA-1  
321 and the sequence was verified and found to be identical. The full-length cDNA was

322 introduced into destination vector pGWPTS1 by recombination from the pENTR/D vector to  
323 make pGWPTS1-AtGAPA-1 (PTS1-GAPA-1) (Supplemental **Fig. S1**). The transgene was  
324 under the control of the *rbcS2B* (1150bp; At5g38420) promoter. In this instance the  
325 expression of the cDNA was under transcriptional control of the Rubisco small subunit 2B  
326 (*rbcS2B*) promoter (At5g38420), which directs high-level photosynthetic tissue specific  
327 transcription of the transgene and followed by the *nos* 3' terminator.

328

### 329 **Generation of transgenic plants**

330 The recombinant plasmid pGWB2-AntiGAPA, pGWB2-AntiGAPB and pGWPTS1-  
331 GAPA-1, were introduced into wild type Arabidopsis by floral dipping (Clough and Bent,  
332 1998) using *Agrobacterium tumefaciens* GV3101. Positive transformants were regenerated on  
333 MS medium containing kanamycin (50mg L<sup>-1</sup>). Kanamycin resistant primary transformants  
334 (T1 generation) with established root systems were transferred to soil and allowed to self-  
335 fertilize. Full details of pGWB2-AntiGAPA, pGWB2-AntiGAPB and PTS1-GAPA-1,  
336 construct assembly can be seen in the Supplemental **Fig. S1**.

337

### 338 **Plant Growth Conditions**

339 For experimental study, T3 progeny seeds from selected lines were germinated on soil  
340 in controlled environment chambers at an irradiance of 130  $\mu\text{mol photons m}^{-2} \text{s}^{-1}$ , 22°C,  
341 relative humidity of 60%, in an 8h/16h square-wave photoperiod. Plants were sown  
342 randomly, and trays rotated daily. Leaf areas were calculated using standard photography and  
343 ImageJ software (imagej.nih.gov/ij). Wild type plants and null segregants (azygous) used in  
344 this study were evaluated independently. Once it was determined that no substantial  
345 differences were observed between these two groups, wild type plants and null segregants  
346 were combined (null segregants from the transgenic lines verified by PCR for non-integration

347 of the transgene) and used as a combined “control” group (CN) (Supplemental Fig. S3). Four  
348 leaf discs (0.6 cm diameter) from two individual leaves, were taken and immediately plunged  
349 into liquid nitrogen, and stored at -80°C for determination of transcript levels by RT-qPCR  
350 and protein content by western blot.

351

### 352 **cDNA generation and RT-qPCR**

353 Total RNA was extracted from Arabidopsis leaf using the NucleoSpin® RNA Plant  
354 Kit (Macherey-Nagel, Fisher Scientific, UK). cDNA was synthesized using 1 µg total RNA  
355 in 20 µl using the oligo-dT primer according to the protocol in the RevertAid Reverse  
356 Transcriptase kit (Fermentas, Life Sciences, UK). cDNA was diluted 1 in 4 to a final  
357 concentration of 12.5ng µL<sup>-1</sup>. For semi quantitative RT-PCR, 2 µL of RT reaction mixture  
358 (100 ng of RNA) in a total volume of 25 µL was used with DreamTaq DNA Polymerase  
359 (Thermo Fisher Scientific, UK) according to manufacturer’s recommendations. For RT-  
360 qPCR, the SensiFAST SYBR No-ROX Kit was used according to manufacturer’s  
361 recommendations (Bioline Reagents Ltd., London, UK). GAPA-1 (At3g26650) and GAPA-2  
362 (At1g12900) transcript were amplified using primers GAPA-F (5’atggttatgggagatgatgg’3)  
363 and GAPA-R (5’ttattggcaacaatgtcagcc’3) and GAPB-F (5’ttcaggtgctctgatgtctctacc’3) and  
364 GAPB-R (5’ tagccactagtgagccaaatccacc’3) respectively.

365

### 366 **Protein Extraction and Western Blotting**

367 Total protein was extracted in extraction buffer (50 mM 4-(2-  
368 Hydroxyethyl)piperazine-1-ethanesulfonic acid (HEPES) pH 8.2, 5 mM MgCl<sub>2</sub>, 1 mM  
369 Ethylenediaminetetraacetic Acid Tetrasodium Salt (EDTA), Glycerol 10% v/v, Triton X-100  
370 0.1% v/v, 2 mM Benzamidine, 2 mM Aminocaproic acid, 0.5 mM Phenylmethanesulfonyl  
371 fluoride (PMSF) and 10 mM DTT). Any insoluble material was removed by centrifugation at

372 14000 g for 10 min (4°C) and protein quantification was determined as previously described  
373 (Harrison et al., 1998; Simkin et al., 2017). Samples were loaded on an equal protein basis,  
374 separated using 12% (w/v) SDS-PAGE, transferred to polyvinylidene difluoride membrane,  
375 and probed using antibodies raised against GAPDH (Pohlmeier et al., 1996). Proteins were  
376 detected using horseradish peroxidase conjugated to the secondary antibody and ECL  
377 chemiluminescence detection reagent (Amersham, Buckinghamshire, UK).

378

### 379 **Chlorophyll fluorescence imaging screening in seedlings**

380 Measurements were performed on 2-week-old Arabidopsis seedlings that had been  
381 grown in a controlled environment chamber at 130  $\mu\text{mol mol}^{-2}\text{s}^{-1}$  PPFD and ambient  
382  $\text{CO}_2$ . Chlorophyll fluorescence parameters were obtained using a chlorophyll fluorescence  
383 (CF) imaging system (Technologica, Colchester, UK (Barbagallo et al., 2003; von  
384 Caemmerer et al., 2004)). The operating efficiency of photosystem two (PSII)  
385 photochemistry,  $F_q'/F_m'$ , was calculated from measurements of steady state fluorescence in  
386 the light ( $F'$ ) and maximum fluorescence in the light ( $F_m'$ ) since  $F_q'/F_m' = (F_m' - F')/F_m'$ .  
387 Images of  $F'$  were taken when fluorescence was stable at 130  $\mu\text{mol m}^{-2} \text{s}^{-1}$  PPFD, whilst  
388 images of maximum fluorescence were obtained after a saturating at 600 ms pulse of 6200  
389  $\mu\text{mol m}^{-2} \text{s}^{-1}$  PPFD (Oxborough and Baker, 2000; Baker et al., 2001; Lawson et al., 2008;  
390 Simkin et al., 2017).

391

### 392 **Gas Exchange Measurements**

393 The response of net photosynthesis ( $A$ ) to intracellular  $\text{CO}_2$  ( $C_i$ ) was measured using a  
394 portable gas exchange system (CIRAS-1, PP Systems Ltd, Ayrshire, UK) as previously  
395 described (Simkin et al., 2017). Leaves were illuminated with an integral red-blue LED light  
396 source (PP systems Ltd, Ayrshire, UK) attached to the gas-exchange system, and light levels



397 were maintained at saturating photosynthetic photon flux density (PPFD) of  $1000 \mu\text{mol m}^{-2} \text{s}^{-1}$   
398  $^1$  for the duration of the  $A/C_i$  response curve. Measurements of  $A$  were made at ambient  $\text{CO}_2$   
399 concentration ( $C_a$ ) at  $400 \mu\text{mol mol}^{-1}$ , before  $C_a$  was decreased to 550, 350, 215,  $60 \mu\text{mol}$   
400  $\text{mol}^{-1}$  before returning to the initial value and increased to 740, 900, 1140, 1340,  $1640 \mu\text{mol}$   
401  $\text{mol}^{-1}$ . Measurements were recorded after  $A$  reached a new steady state (1-2 minutes). Leaf  
402 temperature and vapour pressure deficit (VPD) were maintained at  $25^\circ\text{C}$  and  $1 \pm 0.2 \text{ kPa}$   
403 respectively. The maximum rates of Rubisco- ( $V_{C_{max}}$ ) and the maximum rate of electron  
404 transport for RuBP regeneration ( $J_{max}$ ) were determined and standardized to a leaf  
405 temperature of  $25^\circ\text{C}$  based on equations from von Caemmerer (1981), Bernacchi et al.  
406 (Bernacchi et al., 2001) and Sharkey (2016). All points below 200 ppm were assigned as  
407 rubisco-limited, points above 300 ppm as RuBP-regeneration limited as described (Sharkey,  
408 2016).

409

#### 410 **Statistical Analysis**

411 All statistical analyses were done by comparing ANOVA, using Sys-stat (University  
412 of Essex, UK). The differences between means were tested using the Post hoc Tukey test  
413 (SPSS, Chicago).

#### 414 **Accession numbers**

415 Sequence data from this article can be found in the GenBank/EMBL data libraries under  
416 accession numbers At3g26650 (NM113576) and At1g42970 (AY039961).

417

418

419

420

421

422

423

424 **Funding information**

425 A.J.S, P.E.L.C and L.H were supported by BBSRC (Grant: BB/J004138/1 awarded to  
426 C.A.R). M.A was funded by the Saudi Arabian Government and by the University of Essex  
427 Research Incentive Scheme to C.A.R. A.J.S is supported by the Growing Kent and Medway  
428 Program, UK; Ref 107139.

429

430 **ACKNOWLEDGMENTS**

431 We thank Phillip A. Davey (University of Essex, UK) for help with gas exchange and Tracy  
432 Lawson for help with SigmaPlot.

433

434 **Author Contributions:** A.J.S and M.A generated transgenic plants and performed molecular  
435 and biochemical experiments and carried out plant phenotypic and growth analysis. P.E.L.C  
436 and L.R.H screened and identified GPADH insertion mutants and assisted in experimental  
437 design. M.A performed gas exchange measurement on Arabidopsis. A.J.S and M.A carried  
438 out data analysis on their respective contributions. C.A.R conceived and designed the  
439 research and C.A.R and A.J.S supervised the research. C.A.R, A.J.S wrote the manuscript  
440 with input from all authors.

441

442

ACCEPTED MANUSCRIPT

443 **Tables**

444 **Table I.** *The quantum efficiency of Photosystem II ( $F_q'/F_m'$ ), Maximum electron transport rate ( $J_{max}$ ), the*  
 445 *maximum rate of carboxylation by Rubisco ( $V_{c_{max}}$ ) and maximum assimilation ( $A_{max}$ ) in control and*  
 446 *GAPDH lines in relation to reported protein levels.*

447 Plants were grown in short days at 130  $\mu\text{mol m}^{-2} \text{s}^{-1}$  light intensity, 8 h light/16 h dark cycle. Values represent 4-  
 448 6 plants independent lines (6-8 plants) for group.  $A_{max}$ ,  $V_{c_{max}}$  and  $J_{max}$  derived from  $A/C_i$  response curves shown  
 449 in Figure 3 using the equations published by von Caemmerer and Farquhar (1981) using the spreadsheet  
 450 provided by Sharkey, (2016). ND = not detected. Statistical differences are shown in boldface ( $P < 0.05$ ). SE are  
 451 shown. WT = plants containing Wild Type levels of the transcript and protein subunit. Protein quantities are  
 452 shown in italics.

Line	Relative % <i>GapA</i> transcript and <i>protein</i>	Relative % <i>GapB</i> transcript and <i>protein</i>	$F_q'/F_m'$ 600 $\mu\text{mol m}^{-2} \text{s}^{-1}$	$J_{max}$	$V_{c_{max}}$	$A_{max}$
CN	WT	WT	0.478 +/- 0.014	145.5 +/- 15.75	55.1 +/- 5.2	28.3 +/- 1.15
164	<b>55.2 +/- 15.5</b> <i>51.6 +/- 1.9</i>	WT	0.479 +/- 0.004	<b>89.0 +/- 11.12</b>	<b>40.2 +/- 5.62</b>	<b>16.2 +/- 2.71</b>
cA	<b>9.4 +/- 4.4</b> <i>9.1 +/- 3.7</i>	WT	<b>0.420 +/- 0.014</b>	<b>51.9 +/- 4.41</b>	<b>37.6 +/- 3.19</b>	<b>7.67 +/- 0.91</b>
aA	<b>23.3 +/- 11.8</b> <i>43.6 +/- 5.1</i>	WT	0.449 +/- 0.006	<b>119.7 +/- 7.90</b>	<b>40.2 +/- 2.67</b>	<b>23.4 +/- 1.38</b>
308	WT	ND	0.469 +/- 0.003	<b>101.8 +/- 8.91</b>	56.4 +/- 1.12	<b>18.8 +/- 2.27</b>
aB	WT	<b>22.3 +/- 9.34</b> <i>26.1 +/- 13.8</i>	0.453 +/- 0.004	<b>110.5 +/- 17.12</b>	52.3 +/- 5.92	<b>18.2 +/- 2.34</b> ***
164/ 308	<b>55.2 +/- 15.5</b> <i>51.6 +/- 1.9</i>	ND	<b>0.450 +/- 0.012</b>	<b>101.1 +/- 4.44</b>	<b>38.4 +/- 3.49</b>	<b>20.1 +/- 0.54</b>

453 CN = control. *gapa-1* insertion (164); *gapb* insertion (308); co-suppressed GapA (cA); antisense GapA  
 454 (aA); antisense GapB (aB);

455

456

457 **Figure Legends**

458

459 **Figure 1. Molecular analysis of homozygous GAPDH T-DNA insertion mutants.**

460 Structure of the two GAPDH genes and the location of T-DNA insertions in the (A) *gapa-1*  
 461 (At3g26650; SAIL\_164\_D01) and (B) *gapb* (At1g42970; SAIL\_308\_A06) mutants. Protein-  
 462 coding exons are represented by black and intron locations are displayed as inverted white  
 463 triangles above the coding sequence. Location of genomic PCR-screening primers are shown  
 464 by black arrows on each gene model. T-DNA insertion sites are indicated by triangles below  
 465 the sequence and the precise position is given as the number of base pairs from the ATG.  
 466 ATG, translation initiation codon; TGA, translation termination codon. Bolded G (Panel A)  
 467 and C (Panel B) indicate the point of sequence insertion into the promoter region of the  
 468 SAIL\_164\_D01 and SAIL\_308\_A06 mutants.

469

470 **Figure 2. RT-qPCR and Immunoblot analysis of leaf proteins of wild type and**

471 **experimental GAPDH plants.** (A) Transcript and Protein levels in *gapa-1* (At3g26650;  
 472 SAIL\_164\_D01), GAPA co-suppressed lines (cA), GAPA antisense lines (aA) and control  
 473 (CN). (B) Transcript and Protein levels in *gapb* (At1g42970; SAIL\_308\_A06) and GAPB  
 474 antisense lines (aB). Protein (6 µg) extracts from leaf discs taken from two leaves per plant  
 475 and separated on a 12% acrylamide gel, transferred to membranes and probed with antibodies  
 476 to GAPDH which recognises both GAPA and GAPB subunits. Error bars represent SE of 3  
 477 plants per line.

478

479 **Figure 3. Photosynthetic carbon fixation rate determined as a function of increasing**

480 **CO<sub>2</sub> concentrations (A/Ci) at saturating-light levels (1000 µmol m<sup>-2</sup> s<sup>-1</sup>).** (A) Controls  
 481 (CN) compared to *gapa-1* insertion line (164), GAPA co-suppressed (cA) and GAPA  
 482 antisense (aA) lines. (B) CN compared to *gapb* insertion line (308) and GAPB antisense  
 483 (aB) line lines and (C) Photosynthetic carbon fixation of CN compared to single insertion  
 484 mutants *gapa-1* (164) and *gapb* (308) and the double mutant *gapa-1/gapb* (164/308).  
 485 Extrapolated data are in Table 1. Error bars represent SE of 6 plants per line).

486

487 **Figure 4. Growth analysis of control and experimental lines grown.**

488 grown at 130 µmol m<sup>-2</sup> s<sup>-1</sup> light intensity in short days (8h/16h days) for 52 days. White bar  
 489 represents a size of 6cm. (B) Plant growth rate evaluated over the first 52 days. Lines co-

490 suppressing GAPA (cA), Controls (CN), *gapa-1* insertion mutant (164) and *gapb* insertion  
491 mutant (308) are represented. Results are representative of 9 to 12 plants per line (CN plants  
492 include azygous lines segregated from primary transformants). Significant differences \*  
493 ( $p < 0.10$ ); \*\* ( $p < 0.05$ ); \*\*\* ( $p < 0.01$ ) are indicated. Unless indicated, results are presented as a  
494 percentage of CN (CN = 100%). Error bars represent SE.

495

496 **Figure 5. Growth analysis of control and experimental lines grown in low light.** (A)  
497 *gapa-1* (164) and *gapb* (308) insertion mutants and GAPA co-suppressed (cA), GAPA  
498 antisense (aA) and GAPB (aB) antisense lines were analyzed in parallel. Results are  
499 representative of 8 plants per line. (B) *gapa-1* (164) and *gapb* (308) insertion mutants and the  
500 double mutant *gapa-1/gapb* (164/308) crosses were evaluated. Results are representative of 9  
501 to 12 plants per line. Plants were grown at  $130 \mu\text{mol m}^{-2} \text{s}^{-1}$  light intensity in short days for 46  
502 days. (CN plants include azygous lines segregated from primary transformants). Data were  
503 statistically analysed using 2-way ANOVA. Significant differences \* ( $p < 0.10$ ); \*\* ( $p < 0.05$ );  
504 \*\*\* ( $p < 0.01$ ) are indicated. Results are presented as a percentage of CN (CN = 100%). Error  
505 bars represent SE.

506

507

ACCEPTED MANUSCRIPT

508

509 **References**

510

511 **Baalmann E, Scheibe R, Cerff R, Martin W** (1996) Functional studies of chloroplast  
 512 glyceraldehyde-3-phosphate dehydrogenase subunits A and B expressed in  
 513 *Escherichia coli*: formation of highly active A4 and B4 homotetramers and evidence  
 514 that aggregation of the B4 complex is mediated by the B subunit carboxy terminus.  
 515 *Plant Molecular Biology* **32**: 505-513

516 **Baalmann E, Scheibe R, Cerff R, Martin W** (1996) Functional studies of chloroplast  
 517 glyceraldehyde-3-phosphate dehydrogenase subunits A and B expressed in  
 518 *Escherichia coli*: formation of highly active A4 and B4 homotetramers and evidence  
 519 that aggregation of the B4 complex is mediated by the B subunit carboxy terminus.  
 520 *Plant Mol Biol* **32**: 505-513

521 **Baker NR, Oxborough K, Lawson T, Morison JIL** (2001) High resolution imaging of  
 522 photosynthetic activities of tissues, cells and chloroplasts in leaves. *Journal of*  
 523 *Experimental Botany* **52**: 615-621

524 **Barbagallo RP, Oxborough K, Pallett KE, Baker NR** (2003) Rapid, noninvasive screening  
 525 for perturbations of metabolism and plant growth using chlorophyll fluorescence  
 526 imaging. *Plant Physiology* **132**: 485-493

527 **Bernacchi CJ, Singaas EL, Pimentel C, Portis JAR, Long SP** (2001) Improved  
 528 temperature response functions for models of Rubisco-limited photosynthesis. *Plant*  
 529 *Cell and Environment* **24**: 253-260

530 **Burgess AJ, Masclaux-Daubresse C, Strittmatter G, Weber APM, Taylor SH,**  
 531 **Harbinson J, Yin X, Long S, Paul MJ, Westhoff P, Loreto F, Ceriotti A, Saltenis**  
 532 **VLR, Pribil M, Nacry P, Scharff LB, Jensen PE, Muller B, Cohan J-P, Foulkes**  
 533 **J, Rogowsky P, Debaeke P, Meyer C, Nelissen H, Inzé D, Klein Lankhorst R,**  
 534 **Parry MAJ, Murchie EH, Baekelandt A** (2022) Improving crop yield potential:  
 535 Underlying biological processes and future prospects. *Food and Energy Security* **n/a**:  
 536 e435

537 **Carmo-Silva AE, Marri L, Sparla F, Salvucci ME** (2011) Isolation and compositional  
 538 analysis of a CP12-associated complex of calvin cycle enzymes from *Nicotiana*  
 539 *tabacum*. *Protein and Peptide Letters* **18**: 618-624

540 **Cerff R** (1979) Quaternary structure of higher plant glyceraldehyde-3-phosphate  
 541 dehydrogenases. *Eur J Biochem* **94**: 243-247

542 **Cerff R** (1995) The chimeric nature of nuclear genomes and the antiquity of introns as  
 543 demonstrated by the GAPDH gene system. Elsevier Science

544 **Clough SJ, Bent AF** (1998) Floral dip: a simplified method for *Agrobacterium*-mediated  
 545 transformation of *Arabidopsis thaliana*. *Plant J* **16**: 735-743

546 **Cséke C, Buchanan BB** (1986) Regulation of the formation and utilization of photosynthate  
 547 in leaves. *Biochimica et Biophysica Acta - Reviews on Bioenergetics* **853**: 43-63

548 **De Souza AP, Burgess SJ, Doran L, Hansen J, Manukyan L, Maryn N, Gotarkar D,**  
 549 **Leonelli L, Niyogi KK, Long SP** (2022) Soybean photosynthesis and crop yield are  
 550 improved by accelerating recovery from photoprotection. *Science* **377**: 851-854

551 **Driever SM, Simkin AJ, Alotaibi S, Fisk SJ, Madgwick PJ, Sparks CA, Jones HD,**  
 552 **Lawson T, Parry MAJ, Raines CA** (2017) Increased SBPase activity improves  
 553 photosynthesis and grain yield in wheat grown in greenhouse conditions.  
 554 *Philosophical Transactions of the Royal Society B* **372**: 1730

555 **Fermani S, Sparla F, Falini G, Martelli PL, Casadio R, Pupillo P, Ripamonti A, Trost P**  
 556 (2007) Molecular mechanism of thioredoxin regulation in photosynthetic A2B2-

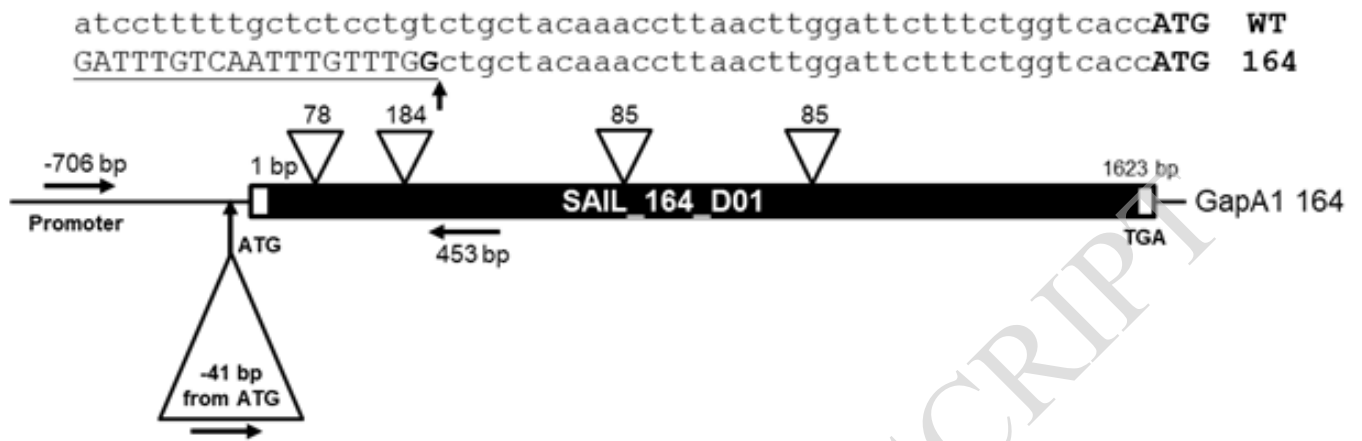
- 557 glycerinaldehyde-3-phosphate dehydrogenase. *Proc Natl Acad Sci U S A* **104**: 11109-  
558 11114
- 559 **Fermani S, Sparla F, Falini G, Martelli PL, Casadio R, Pupillo P, Ripamonti A, Trost P**  
560 (2007) Molecular mechanism of thioredoxin regulation in photosynthetic A2B2-  
561 glycerinaldehyde-3-phosphate dehydrogenase. *Proceedings of the National Academy of*  
562 *Sciences* **104**: 11109-11114
- 563 **Harrison EP, Willingham NM, Lloyd JC, Raines CA** (1998) Reduced sedoheptulose-1,7-  
564 bisphosphatase levels in transgenic tobacco lead to decreased photosynthetic capacity  
565 and altered carbohydrate accumulation. *Planta* **204**: 27-36
- 566 **Howard TP, Lloyd JC, Raines CA** (2011) Inter-species variation in the oligomeric states of  
567 the higher plant Calvin cycle enzymes glycerinaldehyde-3-phosphate dehydrogenase  
568 and phosphoribulokinase. *Journal of Experimental Botany* **62**: 3799-3805
- 569 **Howard TP, Metodiev M, Lloyd JC, Raines CA** (2008) Thioredoxin-mediated reversible  
570 dissociation of a stromal multiprotein complex in response to changes in light  
571 availability. *Proceedings of the National Academy of Sciences* **105**: 4056-4061
- 572 **Iadarola P, Zapponi MC, Ferri G** (1983) Molecular forms of chloroplast glycerinaldehyde-3-  
573 P-dehydrogenase. *Experientia* **39**: 50-52
- 574 **IPCC** (2014) Climate change 2014 impacts, adaptation and vulnerability: Part A: Global and  
575 sectoral aspects: Working group II contribution to the fifth assessment report of the  
576 intergovernmental panel on climate change. *In* VRB C. B. Field, D. J. Dokken, et al.,  
577 eds, ed. Cambridge University Press, Cambridge, UK and New York, NY, USA
- 578 **IPCC** (2019) Summary for Policymakers. *In*: Climate change and land: an IPCC special  
579 report on climate change, desertification, land degradation, sustainable land  
580 management, food security, and greenhouse gas fluxes in terrestrial ecosystems. *In* PR  
581 Shukla, J Skea, E Calvo Buendia, V Masson-Delmotte, HO Pörtner, DC Roberts, P  
582 Zhai, R Slade, S Connors, R Van Diemen, M Ferrat, eds. Cambridge University Press,  
583 Cambridge, UK and New York, NY, USA.
- 584 **Kubis A, Bar-Even A** (2019) Synthetic biology approaches for improving photosynthesis.  
585 *Journal of Experimental Botany* **70**: 1425-1433
- 586 **Lawson T, Lefebvre S, Baker NR, Morison JIL, Raines CA** (2008) Reductions in  
587 mesophyll and guard cell photosynthesis impact on the control of stomatal responses  
588 to light and CO<sub>2</sub>. *Journal of Experimental Botany* **59**: 3609-3619
- 589 **Le Quéré C, Raupach MR, Canadell JG, Marland G, Bopp L, Ciais P, Conway TJ,**  
590 **Doney SC, Feely RA, Foster P, Friedlingstein P, Gurney K, Houghton RA, House**  
591 **JL, Huntingford C, Levy PE, Lomas MR, Majkut J, Metz N, Ometto JP, Peters**  
592 **GP, Prentice IC, Randerson JT, Running SW, Sarmiento JL, Schuster U, Sitch**  
593 **S, Takahashi T, Viovy N, van der Werf GR, Woodward FI** (2009) Trends in the  
594 sources and sinks of carbon dioxide. *Nature Geoscience* **2**: 831-836
- 595 **Lopez-Calcagno PE, Abuzaid AO, Lawson T, Raines CA** (2017) Arabidopsis CP12  
596 mutants have reduced levels of phosphoribulokinase and impaired function of the  
597 Calvin-Benson cycle. *Journal of Experimental Botany* **68**: 2285-2298
- 598 **Lopez-Calcagno PE, Howard TP, Raines CA** (2014) The CP12 protein family: a  
599 thioredoxin-mediated metabolic switch? *Frontiers in Plant Science* **5**: 9
- 600 **Marri L, Trost P, Pupillo P, Sparla F** (2005) Reconstitution and properties of the  
601 recombinant glycerinaldehyde-3-phosphate dehydrogenase/CP12/phosphoribulokinase  
602 supramolecular complex of Arabidopsis. *Plant Physiology* **139**: 1433-1443
- 603 **Nakagawa T, Kurose T, Hino T, Tanaka K, Kawamukai M, Niwa Y, Toyooka K,**  
604 **Matsuoka K, Jinbo T, Kimura T** (2007) Development of series of gateway binary  
605 vectors, pGWBs, for realizing efficient construction of fusion genes for plant  
606 transformation. *J Biosci Bioeng* **104**: 34-41

- 607 NASA (2020) Global climate change: Vital signs of the planet.  
608 <https://climate.nasa.gov/413ppmquotes> *In*,
- 609 **Oxborough K, Baker NR** (2000) An evaluation of the potential triggers of photoinactivation  
610 of photosystem II in the context of a Stern–Volmer model for downregulation and the  
611 reversible radical pair equilibrium model. *Philosophical Transactions of the Royal*  
612 *Society of London. Series B: Biological Sciences* **355**: 1489-1498
- 613 **Pereira LS** (2017) Water, agriculture and food: Challenges and issues. *Water Resources*  
614 *Management* **31**: 2985-2999
- 615 **Pohlmeyer K, Paap BK, Soll J, Wedel N** (1996) CP12: A small nuclear-encoded  
616 chloroplast protein provides novel insights into higher-plant GAPDH evolution. *Plant*  
617 *Molecular Biology Reporter* **32**: 969-978
- 618 **Price GD, Evans JR, von Caemmerer S, Yu JW, Badger MR** (1995) Specific reduction of  
619 chloroplast glyceraldehyde-3-phosphate dehydrogenase activity by antisense RNA  
620 reduces CO<sub>2</sub> assimilation via a reduction in ribulose biphosphate regeneration in  
621 transgenic tobacco plants. *Planta* **195**: 369-378
- 622 **Raines CA** (2022) Improving plant productivity by re-tuning the regeneration of RuBP in the  
623 Calvin–Benson–Bassham cycle. *New Phytologist* **236**: 350-356
- 624 **Raines CA, Cavanagh AP, Simkin AJ** (2022) Chapter 9. Improving carbon fixation. *In* A  
625 Ruban, E Murchie, C Foyer, eds, *Photosynthesis in Action*, Ed 1. Academic Press
- 626 **Ruuska SA, Andrews TJ, Badger MR, Price GD, von Caemmerer S** (2000) The role of  
627 chloroplast electron transport and metabolites in modulating rubisco activity in  
628 tobacco. Insights from transgenic plants with reduced amounts of cytochrome *b/f*  
629 complex or glyceraldehyde 3-phosphate dehydrogenase. *Plant Physiology* **122**: 491-  
630 504
- 631 **Scagliarini S, Trost P, Pupillo P** (1998) The non-regulatory isoform of NAD(P)-  
632 glyceraldehyde-3-phosphate dehydrogenase from spinach chloroplasts. *Journal of*  
633 *Experimental Botany* **49**: 1307-1315
- 634 **Scheibe R, Baalman E, Backhausen JE, Rak C, Vetter S** (1996) C-terminal truncation of  
635 spinach chloroplast NAD(P)-dependent glyceraldehyde-3-phosphate dehydrogenase  
636 prevents inactivation and reaggregation. *Biochim Biophys Acta* **1296**: 228-234
- 637 **Sharkey TD** (2016) What gas exchange data can tell us about photosynthesis. *Plant, Cell &*  
638 *Environment* **39**: 1161-1163
- 639 **Sharkey TD, Bernacchi CJ, Farquhar GD, Singsaas EL** (2007) Fitting photosynthetic  
640 carbon dioxide response curves for C3 leaves. *Plant Cell and Environment* **30**: 1035-  
641 1040
- 642 **Simkin AJ** (2019) Genetic engineering for global food security: photosynthesis and  
643 biofortification. *Plants* **8**: 586
- 644 **Simkin AJ, Lopez-Calcagno PE, Davey PA, Headland LR, Lawson T, Timm S, Bauwe**  
645 **H, Raines CA** (2017) Simultaneous stimulation of sedoheptulose 1,7-bisphosphatase,  
646 fructose 1,6-bisphosphate aldolase and the photorespiratory glycine decarboxylase H-  
647 protein increases CO<sub>2</sub> assimilation, vegetative biomass and seed yield in *Arabidopsis*.  
648 *Plant Biotechnology Journal* **15**: 805-816
- 649 **Simkin AJ, Lopez-Calcagno PE, Raines CA** (2019) Feeding the world: improving  
650 photosynthetic efficiency for sustainable crop production. *Journal of Experimental*  
651 *Botany* **70**: 1119-1140
- 652 **Simkin AJ, McAusland L, Lawson T, Raines CA** (2017) Over-expression of the RieskeFeS  
653 protein increases electron transport rates and biomass yield. *Plant Physiology* **175**:  
654 134-145
- 655 **Sparla F, Pupillo P, Trost P** (2002) The C-terminal extension of glyceraldehyde-3-  
656 phosphate dehydrogenase subunit B acts as an autoinhibitory domain regulated by

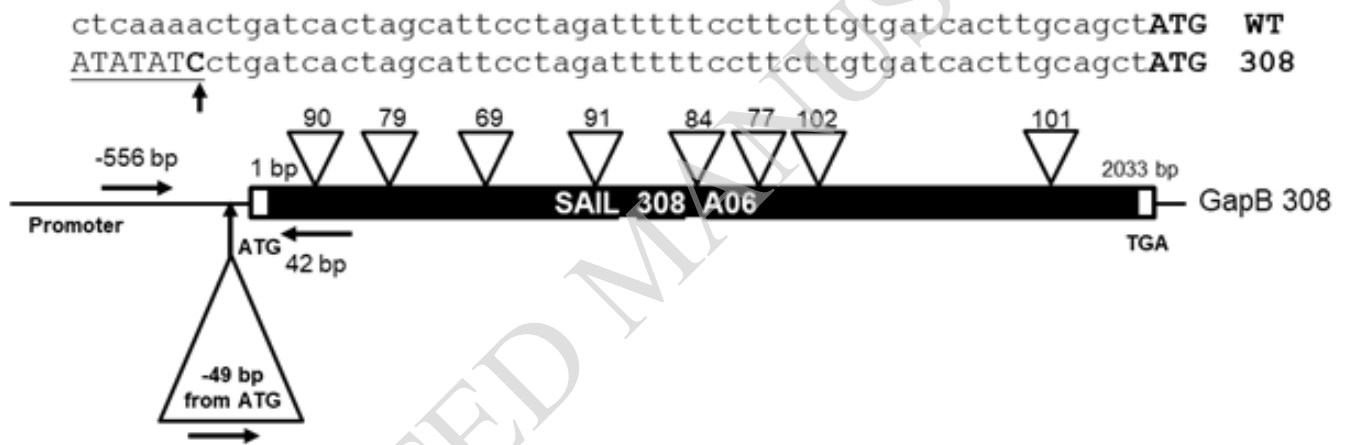


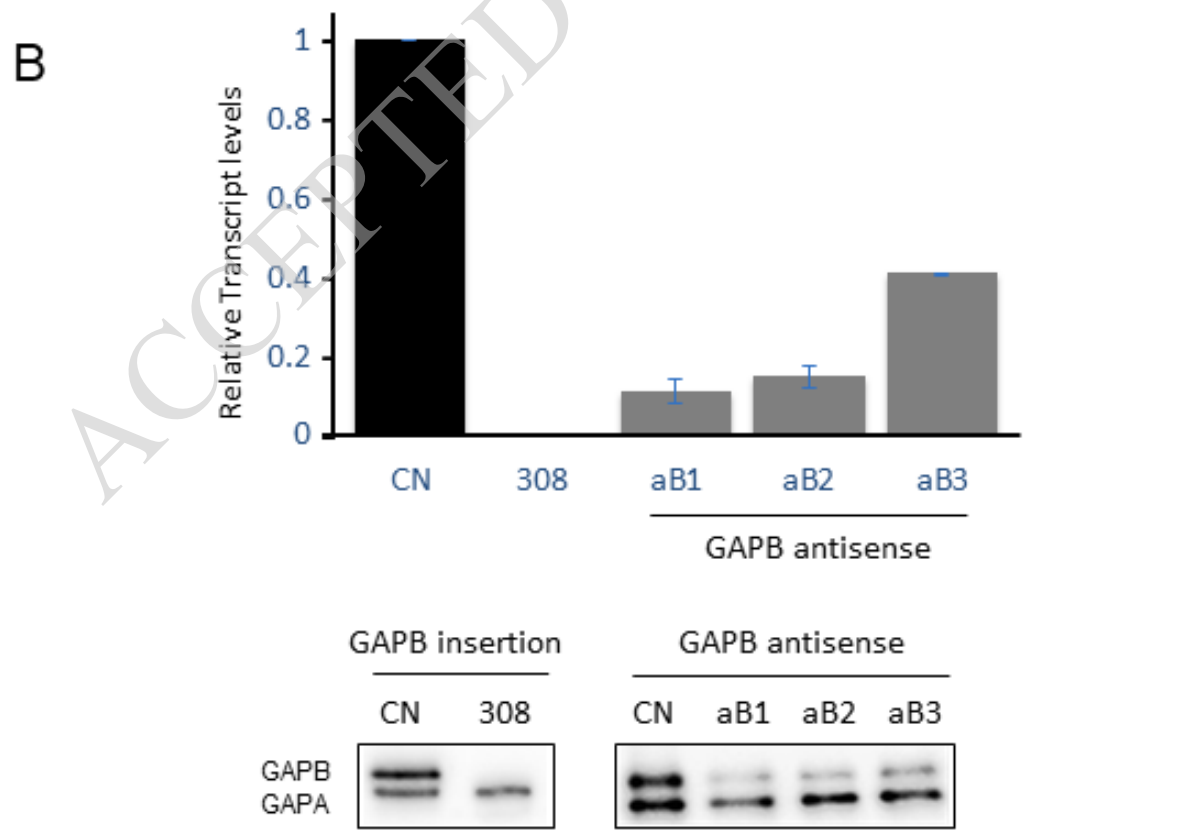
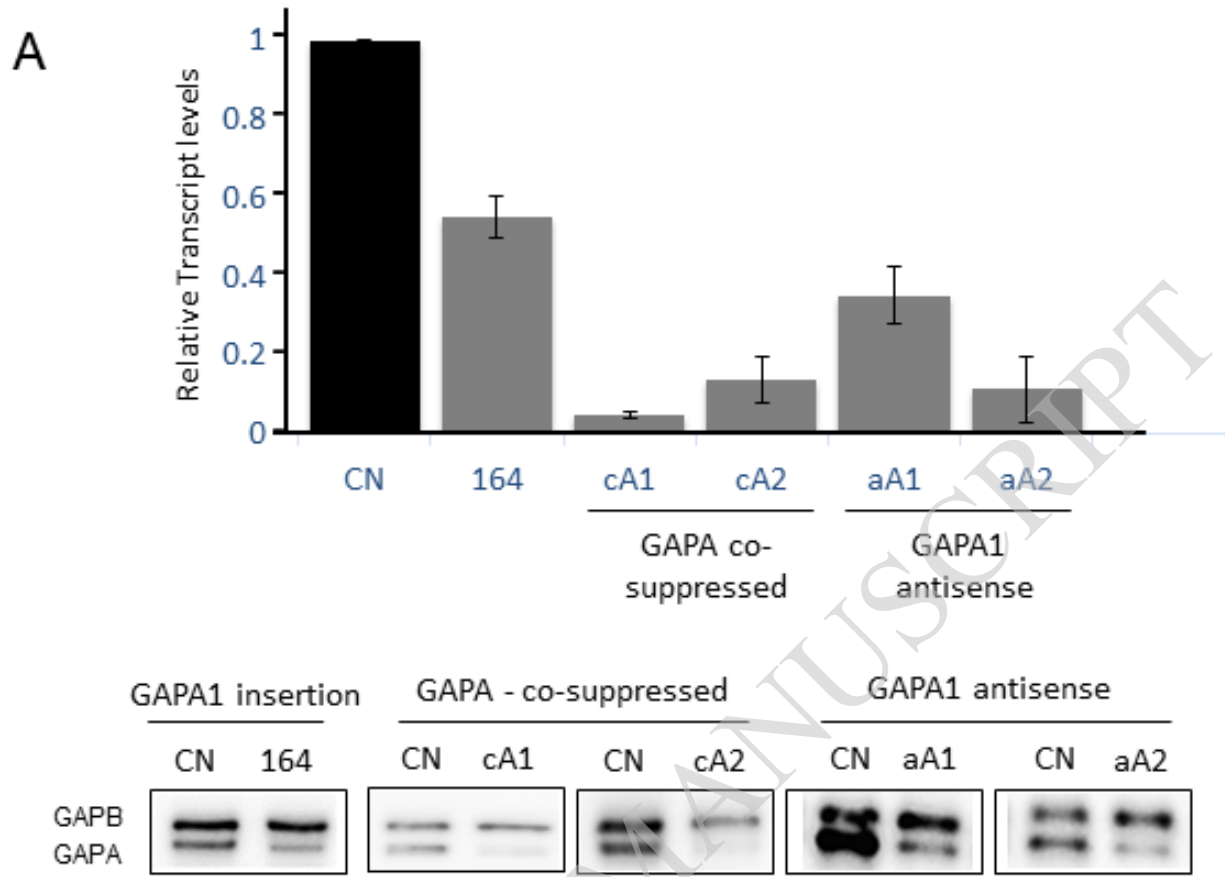
- 657           thioredoxins and nicotinamide adenine dinucleotide. *Journal of Biological Chemistry*  
658           **277**: 44946-44952
- 659   **Sparla F, Zaffagnini M, Wedel N, Scheibe R, Pupillo P, Trost P** (2005) Regulation of  
660   photosynthetic GAPDH dissected by mutants. *Plant Physiology* **138**: 2210-2219
- 661   **Suzuki Y, Ishiyama K, Sugawara M, Suzuki Y, Kondo E, Takegahara-Tamakawa Y,**  
662   **Yoon D-K, Suganami M, Wada S, Miyake C, Makino A** (2021) Overproduction of  
663   chloroplast glyceraldehyde-3-phosphate dehydrogenase improves photosynthesis  
664   slightly under elevated [CO<sub>2</sub>] conditions in rice. *Plant and Cell Physiology* **62**: 156-  
665   165
- 666   **Trost P, Fermani S, Marri L, Zaffagnini M, Falini G, Scagliarini S, Pupillo P, Sparla F**  
667   (2006) Thioredoxin-dependent regulation of photosynthetic glyceraldehyde-3-  
668   phosphate dehydrogenase: autonomous vs. CP12-dependent mechanisms.  
669   *Photosynthesis Research* **89**: 263-275
- 670   **von Caemmerer S, Farquhar GD** (1981) Some relationships between the biochemistry of  
671   photosynthesis and the gas exchange of leaves. *Planta* **153**: 376-387
- 672   **von Caemmerer S, Lawson T, Oxborough K, Baker NR, Andrews TJ, Raines CA** (2004)  
673   Stomatal conductance does not correlate with photosynthetic capacity in transgenic  
674   tobacco with reduced amounts of Rubisco. *J Exp Bot* **55**: 1157-1166
- 675   **Wolosiuk RA, Buchanan BB** (1976) Studies on the regulation of chloroplast NADP-linked  
676   glyceraldehyde-3-phosphate dehydrogenase. *The Journal of Biological Chemistry*  
677   **251**: 6456-6461  
678

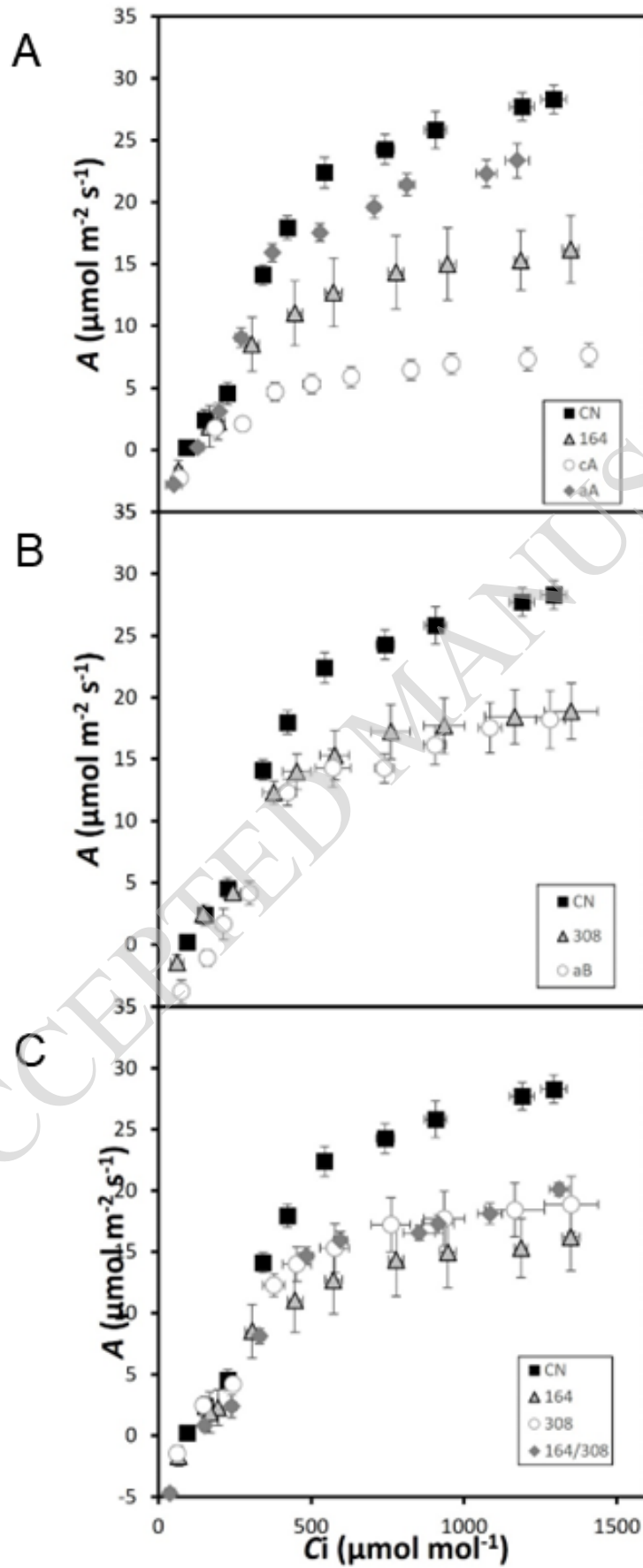
A

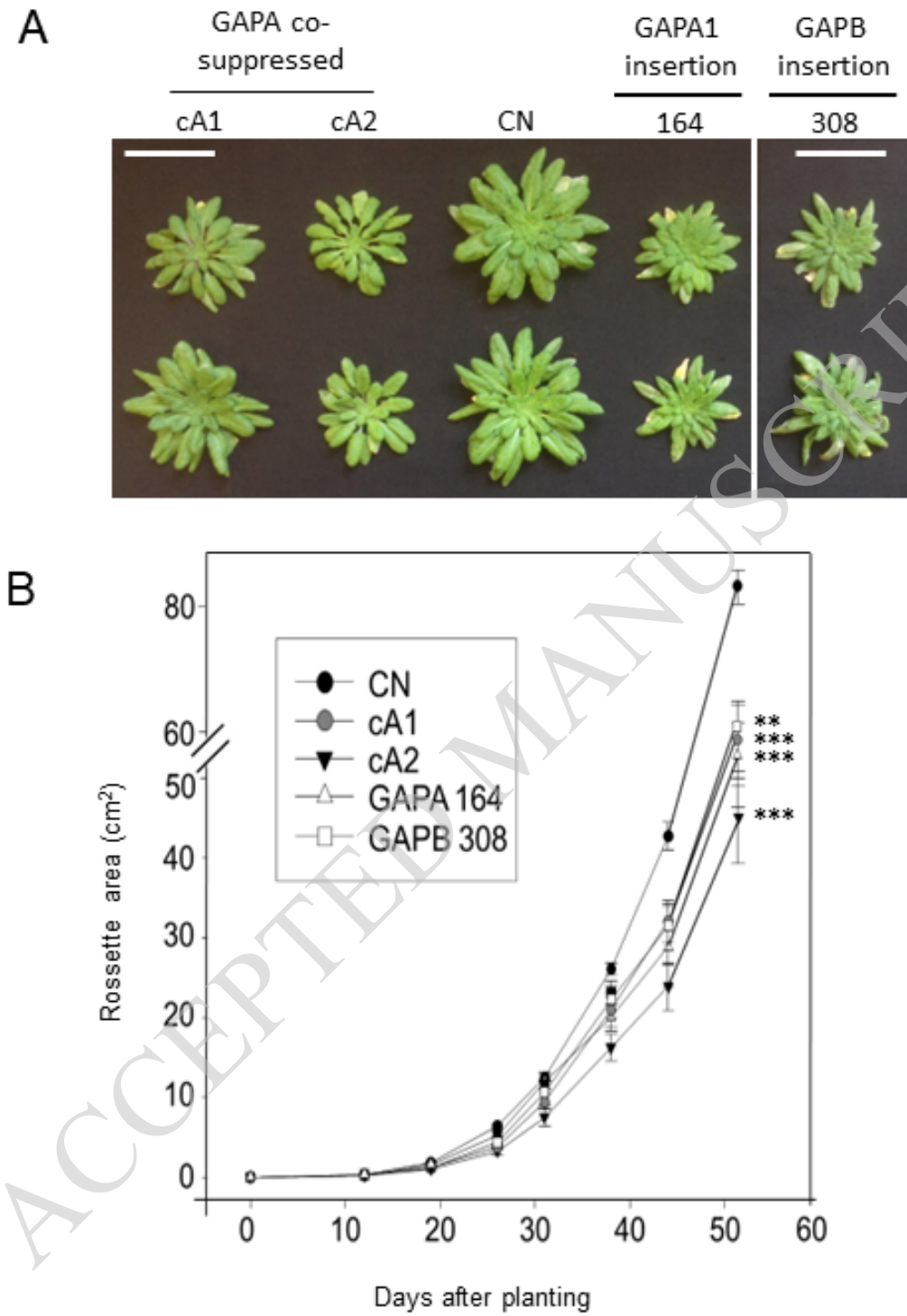


B

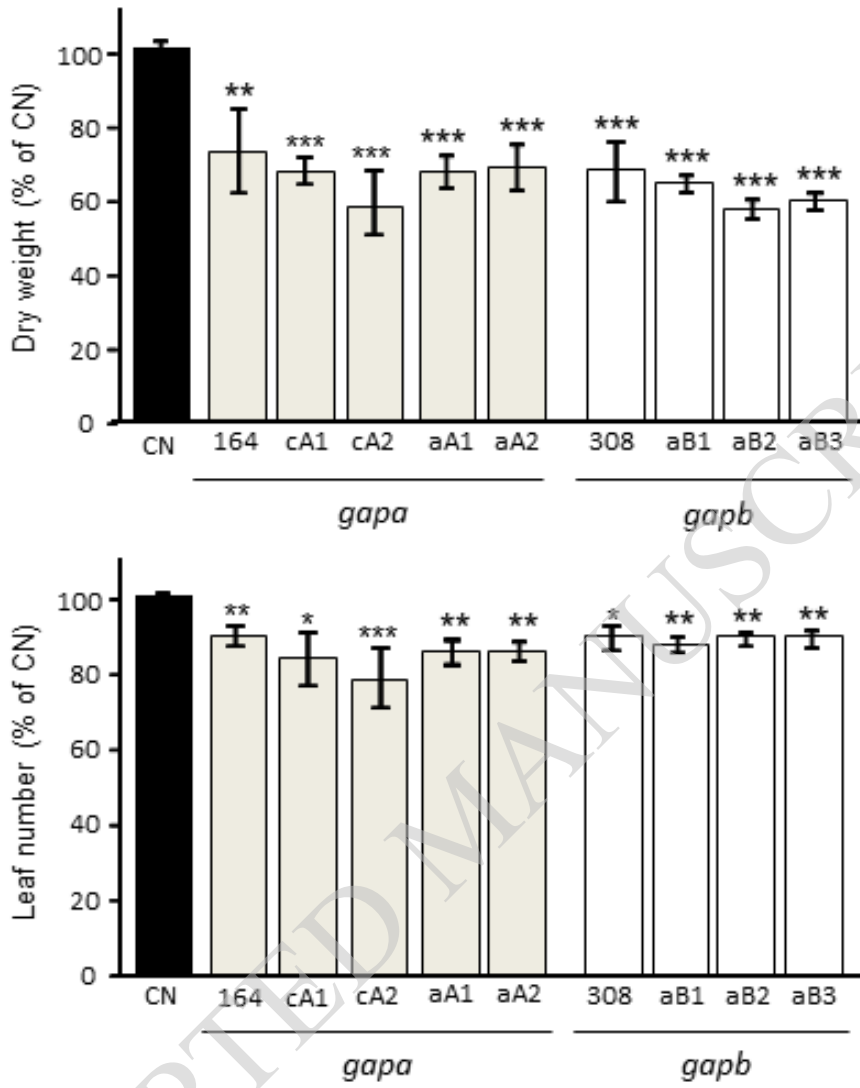




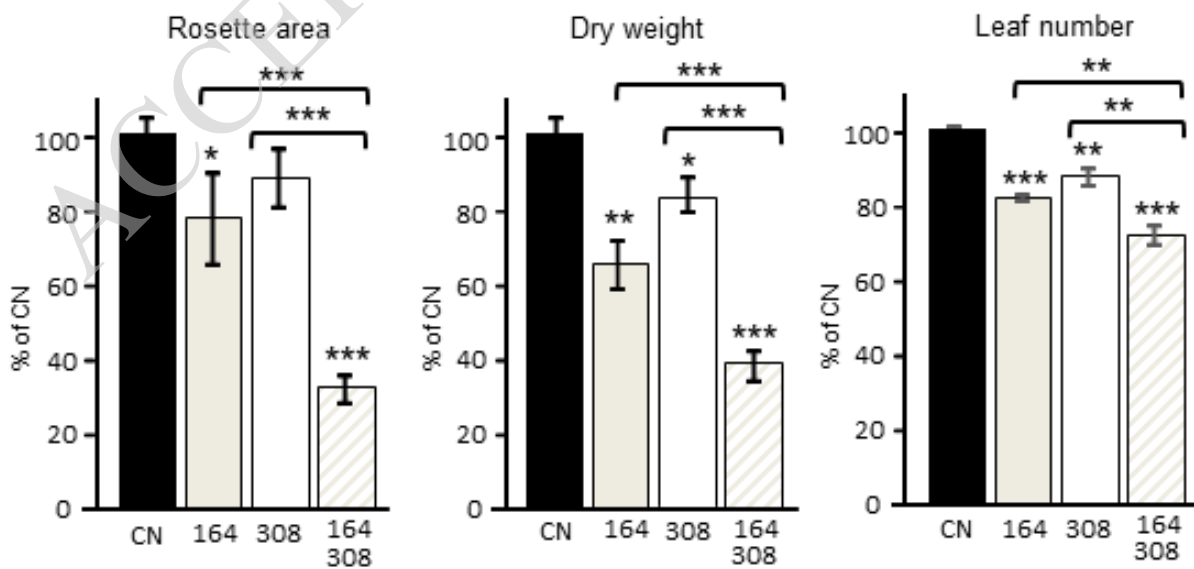




A



B



## Parsed Citations

Baalmann E, Scheibe R, Cerff R, Martin W (1996) Functional studies of chloroplast glyceraldehyde-3-phosphate dehydrogenase subunits A and B expressed in *Escherichia coli*: formation of highly active A4 and B4 homotetramers and evidence that aggregation of the B4 complex is mediated by the B subunit carboxy terminus. *Plant Molecular Biology* 32: 505-513

Google Scholar: [Author Only](#) [Title Only](#) [Author and Title](#)

Baalmann E, Scheibe R, Cerff R, Martin W (1996) Functional studies of chloroplast glyceraldehyde-3-phosphate dehydrogenase subunits A and B expressed in *Escherichia coli*: formation of highly active A4 and B4 homotetramers and evidence that aggregation of the B4 complex is mediated by the B subunit carboxy terminus. *Plant Mol Biol* 32: 505-513

Google Scholar: [Author Only](#) [Title Only](#) [Author and Title](#)

Baker NR, Oxborough K, Lawson T, Morison JIL (2001) High resolution imaging of photosynthetic activities of tissues, cells and chloroplasts in leaves. *Journal of Experimental Botany* 52: 615-621

Google Scholar: [Author Only](#) [Title Only](#) [Author and Title](#)

Barbagallo RP, Oxborough K, Pallett KE, Baker NR (2003) Rapid, noninvasive screening for perturbations of metabolism and plant growth using chlorophyll fluorescence imaging. *Plant Physiology* 132: 485-493

Google Scholar: [Author Only](#) [Title Only](#) [Author and Title](#)

Bernacchi CJ, Singaas EL, Pimentel C, Portis JAR, Long SP (2001) Improved temperature response functions for models of Rubisco-limited photosynthesis. *Plant Cell and Environment* 24: 253-260

Google Scholar: [Author Only](#) [Title Only](#) [Author and Title](#)

Burgess AJ, Masclaux-Daubresse C, Strittmatter G, Weber APM, Taylor SH, Harbinson J, Yin X, Long S, Paul MJ, Westhoff P, Loreto F, Ceriotti A, Saltenis VLR, Pribil M, Nacry P, Scharff LB, Jensen PE, Muller B, Cohan J-P, Foulkes J, Rogowsky P, Debaeke P, Meyer C, Nelissen H, Inzé D, Klein Lankhorst R, Parry MAJ, Murchie EH, Baekelandt A (2022) Improving crop yield potential: Underlying biological processes and future prospects. *Food and Energy Security* n/a: e435

Google Scholar: [Author Only](#) [Title Only](#) [Author and Title](#)

Carmo-Silva AE, Marri L, Sparla F, Salvucci ME (2011) Isolation and compositional analysis of a CP12-associated complex of calvin cycle enzymes from *Nicotiana tabacum*. *Protein and Peptide Letters* 18: 618-624

Google Scholar: [Author Only](#) [Title Only](#) [Author and Title](#)

Cerff R (1979) Quaternary structure of higher plant glyceraldehyde-3-phosphate dehydrogenases. *Eur J Biochem* 94: 243-247

Google Scholar: [Author Only](#) [Title Only](#) [Author and Title](#)

Cerff R (1995) The chimeric nature of nuclear genomes and the antiquity of introns as demonstrated by the GAPDH gene system. *Elsevier Science*

Google Scholar: [Author Only](#) [Title Only](#) [Author and Title](#)

Clough SJ, Bent AF (1998) Floral dip: a simplified method for *Agrobacterium*-mediated transformation of *Arabidopsis thaliana*. *Plant J* 16: 735-743

Google Scholar: [Author Only](#) [Title Only](#) [Author and Title](#)

Cséke C, Buchanan BB (1986) Regulation of the formation and utilization of photosynthate in leaves. *Biochimica et Biophysica Acta - Reviews on Bioenergetics* 853: 43-63

Google Scholar: [Author Only](#) [Title Only](#) [Author and Title](#)

De Souza AP, Burgess SJ, Doran L, Hansen J, Manukyan L, Maryn N, Gotarkar D, Leonelli L, Niyogi KK, Long SP (2022) Soybean photosynthesis and crop yield are improved by accelerating recovery from photoprotection. *Science* 377: 851-854

Google Scholar: [Author Only](#) [Title Only](#) [Author and Title](#)

Driever SM, Simkin AJ, Alotaibi S, Fisk SJ, Madgwick PJ, Sparks CA, Jones HD, Lawson T, Parry MAJ, Raines CA (2017) Increased SBPase activity improves photosynthesis and grain yield in wheat grown in greenhouse conditions. *Philosophical Transactions of the Royal Society B* 372: 1730

Google Scholar: [Author Only](#) [Title Only](#) [Author and Title](#)

Fermani S, Sparla F, Falini G, Martelli PL, Casadio R, Pupillo P, Ripamonti A, Trost P (2007) Molecular mechanism of thioredoxin regulation in photosynthetic A2B2-glyceraldehyde-3-phosphate dehydrogenase. *Proc Natl Acad Sci U S A* 104: 11109-11114

Google Scholar: [Author Only](#) [Title Only](#) [Author and Title](#)

Fermani S, Sparla F, Falini G, Martelli PL, Casadio R, Pupillo P, Ripamonti A, Trost P (2007) Molecular mechanism of thioredoxin regulation in photosynthetic A2B2-glyceraldehyde-3-phosphate dehydrogenase. *Proceedings of the National Academy of Sciences* 104: 11109-11114

Google Scholar: [Author Only](#) [Title Only](#) [Author and Title](#)

Harrison EP, Willingham NM, Lloyd JC, Raines CA (1998) Reduced sedoheptulose-1,7-bisphosphatase levels in transgenic tobacco lead to decreased photosynthetic capacity and altered carbohydrate accumulation. *Planta* 204: 27-36

Google Scholar: [Author Only](#) [Title Only](#) [Author and Title](#)

Howard TP, Lloyd JC, Raines CA (2011) Inter-species variation in the oligomeric states of the higher plant Calvin cycle enzymes glyceraldehyde-3-phosphate dehydrogenase and phosphoribulokinase. *Journal of Experimental Botany* 62: 3799-3805

Google Scholar: [Author Only](#) [Title Only](#) [Author and Title](#)

Howard TP, Metodiev M, Lloyd JC, Raines CA (2008) Thioredoxin-mediated reversible dissociation of a stromal multiprotein complex in response to changes in light availability. *Proceedings of the National Academy of Sciences* 105: 4056-4061

Google Scholar: [Author Only](#) [Title Only](#) [Author and Title](#)

Iadarola P, Zapponi MC, Ferri G (1983) Molecular forms of chloroplast glyceraldehyde-3-P-dehydrogenase. *Experientia* 39: 50-52

Google Scholar: [Author Only](#) [Title Only](#) [Author and Title](#)

IPCC (2014) *Climate change 2014 impacts, adaptation and vulnerability: Part A: Global and sectoral aspects: Working group II contribution to the fifth assessment report of the intergovernmental panel on climate change*. In VRB C. B. Field, D. J. Dokken, et al., eds, ed. Cambridge University Press, Cambridge, UK and New York, NY, USA

Google Scholar: [Author Only](#) [Title Only](#) [Author and Title](#)

IPCC (2019) *Summary for Policymakers*. In: *Climate change and land: an IPCC special report on climate change, desertification, land degradation, sustainable land management, food security, and greenhouse gas fluxes in terrestrial ecosystems*. In PR Shukla, J Skea, E Calvo Buendia, V Masson-Delmotte, HO Pörtner, DC Roberts, P Zhai, R Slade, S Connors, R Van Diemen, M Ferrat, eds. Cambridge University Press, Cambridge, UK and New York, NY, USA

Google Scholar: [Author Only](#) [Title Only](#) [Author and Title](#)

Kubis A, Bar-Even A (2019) Synthetic biology approaches for improving photosynthesis. *Journal of Experimental Botany* 70: 1425-1433

Google Scholar: [Author Only](#) [Title Only](#) [Author and Title](#)

Lawson T, Lefebvre S, Baker NR, Morison JLL, Raines CA (2008) Reductions in mesophyll and guard cell photosynthesis impact on the control of stomatal responses to light and CO<sub>2</sub>. *Journal of Experimental Botany* 59: 3609-3619

Google Scholar: [Author Only](#) [Title Only](#) [Author and Title](#)

Le Quéré C, Raupach MR, Canadell JG, Marland G, Bopp L, Ciais P, Conway TJ, Doney SC, Feely RA, Foster P, Friedlingstein P, Gurney K, Houghton RA, House JI, Huntingford C, Levy PE, Lomas MR, Majkut J, Metz N, Ometto JP, Peters GP, Prentice IC, Randerson JT, Running SW, Sarmiento JL, Schuster U, Sitch S, Takahashi T, Viovy N, van der Werf GR, Woodward FI (2009) Trends in the sources and sinks of carbon dioxide. *Nature Geoscience* 2: 831-836

Google Scholar: [Author Only](#) [Title Only](#) [Author and Title](#)

Lopez-Calcagno PE, Abuzaid AO, Lawson T, Raines CA (2017) Arabidopsis CP12 mutants have reduced levels of phosphoribulokinase and impaired function of the Calvin-Benson cycle. *Journal of Experimental Botany* 68: 2285-2298

Google Scholar: [Author Only](#) [Title Only](#) [Author and Title](#)

Lopez-Calcagno PE, Howard TP, Raines CA (2014) The CP12 protein family: a thioredoxin-mediated metabolic switch? *Frontiers in Plant Science* 5: 9

Marri L, Trost P, Pupillo P, Sparla F (2005) Reconstitution and properties of the recombinant glyceraldehyde-3-phosphate dehydrogenase/CP12/phosphoribulokinase supramolecular complex of Arabidopsis. *Plant Physiology* 139: 1433-1443

Google Scholar: [Author Only](#) [Title Only](#) [Author and Title](#)

Nakagawa T, Kurose T, Hino T, Tanaka K, Kawamukai M, Niwa Y, Toyooka K, Matsuoka K, Jinbo T, Kimura T (2007) Development of series of gateway binary vectors, pGWBs, for realizing efficient construction of fusion genes for plant transformation. *J Biosci Bioeng* 104: 34-41

Google Scholar: [Author Only](#) [Title Only](#) [Author and Title](#)

NASA (2020) *Global climate change: Vital signs of the planet*. <https://climate.nasa.gov/413ppmquotes> In,

Google Scholar: [Author Only](#) [Title Only](#) [Author and Title](#)

Oxborough K, Baker NR (2000) An evaluation of the potential triggers of photoinactivation of photosystem II in the context of a Stern-Volmer model for downregulation and the reversible radical pair equilibrium model. *Philosophical Transactions of the Royal Society of London. Series B: Biological Sciences* 355: 1489-1498

Google Scholar: [Author Only](#) [Title Only](#) [Author and Title](#)

Pereira LS (2017) Water, agriculture and food: Challenges and issues. *Water Resources Management* 31: 2985-2999

Google Scholar: [Author Only](#) [Title Only](#) [Author and Title](#)

Pohlmeyer K, Paap BK, Soll J, Wedel N (1996) CP12: A small nuclear-encoded chloroplast protein provides novel insights into higher-plant GAPDH evolution. *Plant Molecular Biology Reporter* 32: 969-978

Google Scholar: [Author Only](#) [Title Only](#) [Author and Title](#)

Price GD, Evans JR, von Caemmerer S, Yu JW, Badger MR (1995) Specific reduction of chloroplast glyceraldehyde-3-phosphate dehydrogenase activity by antisense RNA reduces CO<sub>2</sub> assimilation via a reduction in ribulose biphosphate regeneration in transgenic tobacco plants. *Planta* 195: 369-378



Google Scholar: [Author Only](#) [Title Only](#) [Author and Title](#)

**Raines CA (2022) Improving plant productivity by re-tuning the regeneration of RuBP in the Calvin–Benson–Bassham cycle. *New Phytologist* 236: 350-356**

Google Scholar: [Author Only](#) [Title Only](#) [Author and Title](#)

**Raines CA, Cavanagh AP, Simkin AJ (2022) Chapter 9. Improving carbon fixation. In A Ruban, E Murchie, C Foyer, eds, *Photosynthesis in Action*, Ed 1. Academic Press**

Google Scholar: [Author Only](#) [Title Only](#) [Author and Title](#)

**Ruuska SA, Andrews TJ, Badger MR, Price GD, von Caemmerer S (2000) The role of chloroplast electron transport and metabolites in modulating rubisco activity in tobacco. Insights from transgenic plants with reduced amounts of cytochrome b/f complex or glyceraldehyde 3-phosphate dehydrogenase. *Plant Physiology* 122: 491-504**

Google Scholar: [Author Only](#) [Title Only](#) [Author and Title](#)

**Scagliarini S, Trost P, Pupillo P (1998) The non-regulatory isoform of NAD(P)-glyceraldehyde-3-phosphate dehydrogenase from spinach chloroplasts. *Journal of Experimental Botany* 49: 1307-1315**

Google Scholar: [Author Only](#) [Title Only](#) [Author and Title](#)

**Scheibe R, Baalman E, Backhausen JE, Rak C, Vetter S (1996) C-terminal truncation of spinach chloroplast NAD(P)-dependent glyceraldehyde-3-phosphate dehydrogenase prevents inactivation and reaggregation. *Biochim Biophys Acta* 1296: 228-234**

Google Scholar: [Author Only](#) [Title Only](#) [Author and Title](#)

**Sharkey TD (2016) What gas exchange data can tell us about photosynthesis. *Plant, Cell & Environment* 39: 1161-1163**

Google Scholar: [Author Only](#) [Title Only](#) [Author and Title](#)

**Sharkey TD, Bernacchi CJ, Farquhar GD, Singaas EL (2007) Fitting photosynthetic carbon dioxide response curves for C3 leaves. *Plant Cell and Environment* 30: 1035-1040**

Google Scholar: [Author Only](#) [Title Only](#) [Author and Title](#)

**Simkin AJ (2019) Genetic engineering for global food security: photosynthesis and biofortification. *Plants* 8: 586**

Google Scholar: [Author Only](#) [Title Only](#) [Author and Title](#)

**Simkin AJ, Lopez-Calcagno PE, Davey PA, Headland LR, Lawson T, Timm S, Bauwe H, Raines CA (2017) Simultaneous stimulation of sedoheptulose 1,7-bisphosphatase, fructose 1,6-bisphosphate aldolase and the photorespiratory glycine decarboxylase H-protein increases CO<sub>2</sub> assimilation, vegetative biomass and seed yield in Arabidopsis. *Plant Biotechnology Journal* 15: 805-816**

Google Scholar: [Author Only](#) [Title Only](#) [Author and Title](#)

**Simkin AJ, Lopez-Calcagno PE, Raines CA (2019) Feeding the world: improving photosynthetic efficiency for sustainable crop production. *Journal of Experimental Botany* 70: 1119-1140**

Google Scholar: [Author Only](#) [Title Only](#) [Author and Title](#)

**Simkin AJ, McAusland L, Lawson T, Raines CA (2017) Over-expression of the RieskeFeS protein increases electron transport rates and biomass yield. *Plant Physiology* 175: 134-145**

Google Scholar: [Author Only](#) [Title Only](#) [Author and Title](#)

**Sparla F, Pupillo P, Trost P (2002) The C-terminal extension of glyceraldehyde-3-phosphate dehydrogenase subunit B acts as an autoinhibitory domain regulated by thioredoxins and nicotinamide adenine dinucleotide. *Journal of Biological Chemistry* 277: 44946-44952**

Google Scholar: [Author Only](#) [Title Only](#) [Author and Title](#)

**Sparla F, Zaffagnini M, Wedel N, Scheibe R, Pupillo P, Trost P (2005) Regulation of photosynthetic GAPDH dissected by mutants. *Plant Physiology* 138: 2210-2219**

Google Scholar: [Author Only](#) [Title Only](#) [Author and Title](#)

**Suzuki Y, Ishiyama K, Sugawara M, Suzuki Y, Kondo E, Takegahara-Tamakawa Y, Yoon D-K, Suganami M, Wada S, Miyake C, Makino A (2021) Overproduction of chloroplast glyceraldehyde-3-phosphate dehydrogenase improves photosynthesis slightly under elevated [CO<sub>2</sub>] conditions in rice. *Plant and Cell Physiology* 62: 156-165**

Google Scholar: [Author Only](#) [Title Only](#) [Author and Title](#)

**Trost P, Fermani S, Marri L, Zaffagnini M, Falini G, Scagliarini S, Pupillo P, Sparla F (2006) Thioredoxin-dependent regulation of photosynthetic glyceraldehyde-3-phosphate dehydrogenase: autonomous vs. CP12-dependent mechanisms. *Photosynthesis Research* 89: 263-275**

Google Scholar: [Author Only](#) [Title Only](#) [Author and Title](#)

**von Caemmerer S, Farquhar GD (1981) Some relationships between the biochemistry of photosynthesis and the gas exchange of leaves. *Planta* 153: 376-387**

Google Scholar: [Author Only](#) [Title Only](#) [Author and Title](#)

**von Caemmerer S, Lawson T, Oxborough K, Baker NR, Andrews TJ, Raines CA (2004) Stomatal conductance does not correlate with photosynthetic capacity in transgenic tobacco with reduced amounts of Rubisco. *J Exp Bot* 55: 1157-1166**

Google Scholar: [Author Only](#) [Title Only](#) [Author and Title](#)

**Wolosiuk RA, Buchanan BB (1976) Studies on the regulation of chloroplast NADP-linked glyceraldehyde-3-phosphate dehydrogenase. The Journal of Biological Chemistry 251: 6456-6461**

Google Scholar: [Author Only](#) [Title Only](#) [Author and Title](#)

ACCEPTED MANUSCRIPT